Available online at www.sciencedirect.com

SCIENCE DIRECT

Cement and Concrete Research 36 (2006) 3 – 17

Cement and Concrete Research

A new aluminium-hydrate species in hydrated Portland cements characterized by ^{27}Al and ^{29}Si MAS NMR spectroscopy

Morten Daugaard Andersen, Hans J. Jakobsen, Jørgen Skibsted*

Instrument Centre for Solid-State NMR Spectroscopy, Department of Chemistry, University of Aarhus, DK-8000 Aarhus C, Denmark

Received 27 August 2004; accepted 11 April 2005

Abstract

Recent ^{27}Al MAS NMR studies of hydrated Portland cements and calcium-silicate-hydrate (C-S-H) phases have shown a resonance from Al in octahedral coordination, which cannot be assigned to the well-known aluminate species in hydrated Portland cements. This resonance, which exhibits the isotropic chemical shift $\delta_{iso}=5.0$ ppm and the quadrupole product parameter $P_Q=1.2$ MHz, has been characterized in detail by ^{27}Al MAS and ^{27}Al{^{1}H} CP/MAS NMR for different hydrated white Portland cements and C-S-H phases. These experiments demonstrate that the resonance originates from an amorphous or disordered aluminate hydrate which contains $Al(OH)_6^{3-}$ or $O_xAl(OH)_{6-x}^{(3+x)-}$ units. The formation of the new aluminate hydrate is related to the formation of C-S-H at ambient temperatures, however, it decomposes by thermal treatment at temperatures of 70–90 °C. From the experiments in this work it is proposed that the new aluminate hydrate is either an amorphous/disordered aluminate hydroxide or a calcium aluminate hydrate, produced as a separate phase or as a nanostructured surface precipitate on the C-S-H phase. Finally, the possibilities of Al^{3+} for Ca^{2+} substitution in the principal layers and interlayers of the C-S-H structure are discussed.

Keywords: Amorphous material; Calcium-silicate-hydrate (C-S-H); Hydration products; Spectroscopy; Portland cement

1. Introduction

Ordinary and white Portland cements typically have a bulk Al_2O_3 content in the range 1–6 wt.% with aluminium mainly present in the calcium aluminate ($Ca_3Al_2O_6$) and aluminoferrite ($Ca_2Al_xFe_{2-x}O_5$, $0 \le x \le 1.4$) phases [1]. Furthermore, it is well-known that a considerable fraction of the aluminium is present as Al^{3+} guest-ions in the calcium silicate phases alite and belite [1,2]. During hydration of Portland cements the principal hydration products of the calcium aluminate and aluminoferrite phases are the AFt and AFm phases ettringite ($Ca_6[Al(OH)_6]_2(SO_4)_3{\cdot}26H_2O$) and monosulphate ($Ca_4[Al(OH)_6]_2SO_4{\cdot}6H_2O$), while hydrogarnet ($Ca_3[Al(OH)_6]_2$) may form with insufficiently added gypsum. However, depending on the physical conditions and chemical environments during cement hydration, other AFm and AFt phases such as $Ca_2[Al(OH)_6]OH{\cdot}xH_2O$ ($x=0$, 2, 3, 6) [3], Friedels salt ($Ca_2[Al(OH)]_6Cl{\cdot}2H_2O$), and the carbonate analogues of ettringite and monosulphate can also be formed [1]. A general feature for these aluminate hydrates is that they all contain aluminium in octahedral coordination. Moreover, a significant quantity of aluminium is incorporated in the calcium-silicate-hydrate (C-S-H) phase, where AlO_4 units take part in the tetrahedral chain structure of SiO_4 tetrahedra [4–6]. For C-S-H phases with high Ca/Si ratios, it has also been proposed that Al may be incorporated in the interlayer region of the C-S-H structure, potentially by substitution for interlayer Ca^{2+} ions, forming AlO_6 octahedra [7–10].

Considering the low Al_2O_3 content of Portland cements, it can be hard to identify the abovementioned aluminate phases, even though some of them are present in a crystalline form, since they may be present in quantities less than 1 wt.% of the hydrated Portland cement. For this

* Corresponding author. Tel.: +45 8942 3900; fax: +45 8619 6199.
E-mail address: jskib@chem.au.dk (J. Skibsted).

0008-8846/$ - see front matter © 2005 Elsevier Ltd. All rights reserved.
doi:10.1016/j.cemconres.2005.04.010

purpose, ^{27}Al MAS NMR spectroscopy represents a unique analytical tool because of the high sensitivity for the ^{27}Al nucleus (e.g., 100% natural abundance and a high gyromagnetic ratio). The potential of ^{27}Al MAS NMR in studies of Portland cements was demonstrated in a preliminary investigation of a white Portland cement [11], where the hydration of the calcium aluminate phase could be followed by the distinction of tetrahedrally and octahedrally coordinated Al species. In a subsequent investigation of synthetic samples of the aluminate phases in Portland cements, the ^{27}Al quadrupole coupling parameters (C_Q and η_Q) and isotropic chemical shifts (δ_{iso}) were determined for the individual Al sites with good precision [12], thereby providing the tool for detection and quantification of Al in for example ettringite and monosulphate. ^{27}Al MAS NMR has also been widely used to characterize the incorporation of Al in C-S-H samples [7,8,10,13,14], in C-S-H phases resulting from activated slag cements [5,15], and in the C-S-H of hydrated Portland cements [6,16]. The high sensitivity of ^{27}Al MAS NMR can be illustrated by the results from a recent ^{27}Al MAS NMR study of a white Portland cement (1.74 wt.% Al_2O_3) hydrated for 28 days, which was found to contain 3.2 wt.% ettringite, 1.2 wt.% monosulphate, and a quantity of tetrahedral Al incorporated in the C-S-H phase corresponding to 0.12 wt.% Al_2O_3 [16].

In this work we investigate the origin of a third resonance from Al in octahedral coordination which has recently been observed in ^{27}Al MAS NMR spectra of hydrated white Portland cements [6,16] in addition to the resonances from ^{27}Al in ettringite and monosulphate. A similar resonance has also been reported in ^{27}Al MAS NMR spectra of Al-substituted C-S-H samples [9,10,13] and tentatively assigned to Al substituting for Ca in the principal layers of composition CaO_2 in the C-S-H [10] or the incorporation of Al in an octahedral site in the C-S-H interlayer [9,13]. However, the results in the present work show that the third Al_{VI} resonance originates from an amorphous or disordered, nanoscale aluminate-hydrate which is formed either as a separate phase or as a surface precipitate on the C-S-H material. Thus, we have denoted this species as the *third aluminate hydrate* (*TAH*), since it is formed in addition to the ettringite (AFt) and monosulphate (AFm) aluminate hydrates. The TAH species is formed in hydrated Portland cements in very small quantities, corresponding to an equivalent quantity of 0.1–0.5 wt.% Al_2O_3. This fact and the amorphous/disordered nature of TAH may be the reason that it has not been observed by other analytical techniques such as X-ray diffraction. Because solid-state NMR spectra primarily reflects the first- and second-coordination spheres of the spin nucleus under investigation, it has at the present time not been possible to obtain the constitutional formula for TAH but only to establish the local environment of the Al units and its thermal stability. Moreover, it is noted that this study focuses on the formation of TAH in two white Portland cements, having a low and high Al_2O_3 content, because the low quantities of paramagnetic ions (e.g., Fe^{3+}) in these cements only result in minimal line broadening of the NMR resonances caused by nuclear-electron dipolar couplings between ^{27}Al (^{29}Si) and the unpaired electron of the Fe^{3+} ions.

2. Experimental

2.1. Materials and sample preparation

The white Portland cements were commercial cements produced by Aalborg Portland A/S, Denmark and Sinai White Cement Company, Egypt with the bulk metal oxide compositions given in Table 1 and with a Blaine fineness of 424 m^2/kg and 389 m^2/kg, respectively. The main difference between these cements is that the Aalborg cement contains a small quantity of Al_2O_3 while the Sinai cement has a high Al_2O_3 content for a white Portland cement. A sample of white Portland clinkers from Aalborg Portland A/S, with the oxide composition listed in Table 1, was also investigated. Gypsum ($CaSO_4{\cdot}2H_2O$, 99% purity) was obtained from Merck (Darmstadt, Germany) and used as received.

Table 2 summarizes the composition of the eight series of hydration which were prepared using the white Portland cements/clinkers and in some cases gypsum as an additive. All hydration mixtures employed a water/cement or water/powder ratio of 0.50, triple distilled water, and a hydration temperature of 20 °C. The cements and additives were mixed with water by hand for about 5 min. Subsequently, the samples were placed in open plastic bags in a desiccator with a relative humidity of 100% at 20 °C. At specific curing times a part of the pastes was ground to a fine powder and the hydration process was stopped by stirring the sample in acetone for 15 min. The powdered samples were dried in a desiccator over silica gel at room temperature and stored in airtight containers to prevent contamination from atmospheric CO_2. Four samples of *C1_H* hydrated for 3 years were heated for 24 h at temperatures from 70 to 200 °C.

The C-S-H samples were prepared from analytically pure $Ca(OH)_2$ (Riedel-de Haën), SiO_2 (Cab-osil, M5, Riedel-de Haën), and $NaAlO_2$ (Strem Chemicals). The solids were

Table 1
Bulk oxide composition for the white Portland cements (wPc) and clinkers produced by Aalborg Portland A/S and Sinai White Cement Company

Oxide (wt.%)	wPc-Aalborg	wPc-Sinai	white clinkers (Aalborg)
CaO	69.13	67.10	70.43
SiO_2	24.70	22.39	25.88
Al_2O_3	1.74	4.28	1.97
Fe_2O_3	0.31	0.30	0.33
MgO	0.56	0.19	0.59
SO_3	1.97	2.72	0.17
K_2O	0.05	0.02	–
Na_2O	0.16	0.04	–
Loss on ignition	0.99	2.72	–

Table 2
Series of hydration for the white Portland cements (wPc) and clinkers studied in this work[a]

Index	Cement type[b]	Additive
C1_H	wPc-Aalborg	
C2_2G	wPc-Aalborg	2.0 wt.% gypsum
C3_5G	wPc-Aalborg	5.0 wt.% gypsum
C4_SH	wPc-Sinai	
CL5_H	White clinker, Aalborg	
CL6_2G	White clinker, Aalborg	2.0 wt.% gypsum
CL7_5G	White clinker, Aalborg	5.0 wt.% gypsum
CL8_10G	White clinker, Aalborg	10.0 wt.% gypsum

[a] All series employed the water/powder ratio w/p=0.50 and were stored at 20 °C and a relative humidity of 100% during hydration.
[b] The oxide composition of the cements/clinkers are given in Table 1.

mixed with triple distilled water, employing a water/solid ratio of 50, and stored at room temperature for 3 weeks in closed glass tubes with continuous stirring. The suspensions were filtered and the precipitates were subsequently dried in a desiccator over silica gel at room temperature. The synthesis employed the initial ratio $(Al/Si)_i=0.05$ and initial Ca/Si ratios of $(Ca/Si)_i=0.66$, 0.83, 1.00, 1.25, 1.50, and 1.75.

2.2. NMR measurements

Solid-state ^{27}Al MAS NMR experiments were performed on Varian *Unity* INOVA 300 MHz (7.05 T), 400 MHz (9.39 T), and 600 MHz (14.09 T) spectrometers using home-built CP/MAS probes for 4 and 5 mm o.d. zirconia (PSZ) rotors. The single-pulse ^{27}Al MAS NMR spectra obtained at 7.05 and 9.39 T were acquired with a pulse width of 0.5 μs for an rf field strength of $\gamma B_1/2\pi=60$ kHz (i.e., a flip angle $<\pi/6$ for ^{27}Al, $I=5/2$, in a solid) to ensure quantitative reliability of the intensities observed for the ^{27}Al central transition for sites experiencing different quadrupole couplings. Moreover, the experiments employed ^{1}H decoupling with $\gamma B_2/2\pi=75$ kHz, spinning speeds of about $\nu_R\approx10$ kHz, a 2-s relaxation delay, and typically 10,000 scans. The ^{27}Al MAS NMR spectra at 14.09 T were obtained in a similar manner employing $\gamma B_1/2\pi=50$ kHz, $\gamma B_2/2\pi=50$ kHz, and $\nu_R=13.0$ kHz. At the three magnetic fields, the ^{27}Al MAS NMR spectrum of the probe itself with an empty spinning ($\nu_R=10.0-13.0$ kHz) PSZ rotor showed a broad resonance of very low intensity. This spectrum was subtracted from the ^{27}Al MAS NMR spectra of the cement samples prior to the quantitative evaluation of the observed intensities. The quantities of the different aluminate phases were determined from ^{27}Al MAS NMR spectra of weighed samples using the ^{27}Al MAS NMR spectrum of a weighed sample of α-Al_2O_3 as an external intensity reference. The ^{27}Al MAS NMR spectrum at 21.15 T was obtained on a Varian INOVA-900 spectrometer at Oxford Instruments, U.K., using a home-built 900 MHz CP/MAS NMR probe [17] and a pulse width of $\tau_p=1.0$ μs for $\gamma B_1/2\pi=60$ kHz. The $^{27}Al\{^{1}H\}$ cross-polarization (CP) MAS experiments (9.39 T) used high-power ^{1}H decoupling ($\gamma B_2/2\pi=58$ kHz), a fixed rf field strength of $\nu_{rf}(^{1}H)=\gamma B_2/2\pi=56$ kHz, and an array of ^{27}Al rf field strengths in the range $\nu_{rf}(^{27}Al)=\gamma B_1/2\pi=18-57$ kHz during the CP contact time which was varied from 50 μs to 5.0 ms.

Solid-state ^{29}Si MAS NMR spectra were recorded at 79.4 MHz on a Varian INOVA-400 (9.39 T) spectrometer using a home-built CP/MAS probe for 7 mm o.d. PSZ rotors (220 μL sample volume) and a spinning speed of $\nu_R=6.0$ kHz. The ^{29}Si MAS experiments employed an rf field strength of $\gamma B_1/2\pi=40$ kHz, a pulse width of 3 μs, a relaxation delay of 30 s, and typically 2048 scans. These conditions were found to give quantitative reliable intensities in the ^{29}Si MAS NMR spectra of hydrated white Portland cements. ^{29}Si and ^{27}Al chemical shifts are referenced to external samples of tetramethylsilane (TMS) and a 1.0 M aqueous solution of $AlCl_3{\cdot}6H_2O$, respectively. Simulations of the ^{27}Al MAS NMR spectra employed the STARS solid-state NMR software package, developed earlier in our laboratory [18], while the deconvolutions of the ^{29}Si MAS spectra were performed with the Varian Vnmr software.

3. Results and discussion

3.1. High-field ^{27}Al MAS NMR

The current status for ^{27}Al MAS NMR spectroscopy in studies of cementitious materials is that the highest degree of resolution for resonances from different aluminate species is achieved using the standard single-pulse MAS experiment at high magnetic fields ($B_0\sim14-21$ T) combined with high-power ^{1}H decoupling ($\gamma B_2/2\pi\geq50$ kHz) and high-speed spinning ($\nu_R\geq10$ kHz). This is primarily due to the high sensitivity of this experiment for low quantities of aluminium as well as the increased chemical shift dispersion and reduced second-order quadrupole broadening with increasing magnetic field strength. It is noted that the two-dimensional ^{27}Al multiple-quantum (MQ)MAS experiment, which removes the second-order quadrupole broadening in one dimension, has only provided new information about cementitious materials in a very few applications [14,19].

Fig. 1 illustrates ^{27}Al MAS NMR spectra of the central transition ($m=1/2\leftrightarrow m=-1/2$), recorded under the above-mentioned conditions, for two different white Portland cements (*C1_H* and *C4_SH*) and white Portland clinkers (*CL5_H*) hydrated for 2 weeks. The chemical shift region for Al in tetrahedral coordination ($50\leq\delta\leq100$ ppm) displays centerbands from (i) Al incorporated in alite/belite with a center of gravity $\delta^{cg}_{1/2,-1/2}\approx86$ ppm [2], (ii) Al in an impure form of tricalcium aluminate ($\delta^{cg}_{1/2,-1/2}\approx81$ ppm [12]), and (iii) Al substituting for Si in the C-S-H phase ($\delta^{cg}_{1/2,-1/2}\approx75$ ppm [5,6]). At lower frequency, a broadened resonance with low intensity is observed at $\delta^{cg}_{1/2,-1/2}\approx35$ ppm, which has tentatively been ascribed to a five-fold coordinated Al site that originates from Al^{3+} substituting for Ca^{2+} ions situated

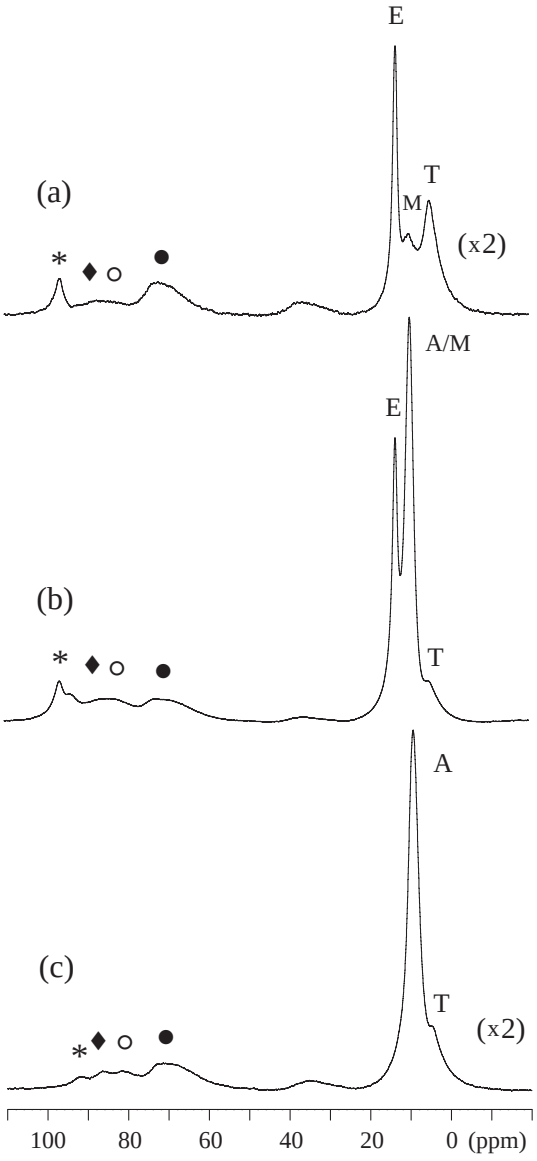

Fig. 1. ^{27}Al MAS NMR spectra (14.1 T, 13.0 kHz) obtained with high-power ^{1}H decoupling of the central transition for (a) *C1_H*, (b) *C4_SH*, and (c) *CL5_H* all hydrated for 2 weeks. The asterisks (*) indicate spinning sidebands whereas the filled diamond (♦) and the open circle (○) show the centerbands from Al incorporated in alite/belite and Al in the calcium aluminate phase $Ca_3Al_2O_6$, respectively. The filled circle (●) indicates the centerband for tetrahedrally coordinated Al incorporated in the C-S-H phase while the centerbands from ettringite, monosulphate, calcium aluminate hydrate, and the third aluminate hydrate (TAH) are denoted by E, M, A, and T, respectively. A vertical expansion by a factor of two is employed for the spectra in (a) and (c) as compared to the spectrum in (b).

in the interlayers of the C-S-H structure [10] (*vide infra*). The spectral region for octahedrally coordinated Al ($-10 \leq \delta \leq 20$ ppm) exhibits three distinct resonances, where the high-frequency peak ($\delta_{iso} = 13.1$ ppm) can be unambiguously assigned to ettringite [12]. The second resonance has a center of gravity $\delta^{cg}_{1/2,-1/2} \approx 9.8$ ppm, in accordance with the quadrupole coupling and chemical shift parameters reported for monosulphate [12]. However, other AFm phases such as $Ca_2[Al(OH)_6]OH{\cdot}6H_2O$ and Friedels salt have very similar quadrupole coupling and chemical shift parameters [12,20] and thus, these phases cannot be distinguished by ^{27}Al MAS NMR under the actual experimental conditions. Finally, a third resonance is observed at $\delta^{cg}_{1/2,-1/2} \approx 5$ ppm with a linewidth similar to that for monosulphate. This resonance cannot be assigned to any of the known aluminate phases, which may be present in hydrated Portland cements and thus, we ascribe this resonance to a hitherto unknown aluminate hydrate (TAH) formed in hydrated Portland cements. Quantification of the intensities in the ^{27}Al MAS NMR spectra combined with deconvolution of the spectral region for octahedrally coordinated Al give equivalent quantities of Al_2O_3 of 0.32 ± 0.05 wt.%, 0.19 ± 0.05 wt.%, and 0.12 ± 0.05 wt.% in the third aluminate hydrate (TAH) for the *C1_H*, *C4_SH*, and *CL5_H* samples, respectively, demonstrating that this species is present in very small quantities. The Al_2O_3 quantities for TAH in the three cements do not show any correlation with the bulk Al_2O_3 contents of the cements (c.f., Table 1). Furthermore, the degree of hydration for alite and belite, determined from ^{29}Si MAS NMR, is quite similar for the three cements, which shows the absence of a direct relationship between the quantity of TAH and the amount of C-S-H formed in the hydrated cements. However, for each of the three cements, the quantity of TAH increases with increasing hydration time (*vide infra*).

3.2. ^{27}Al quadrupole coupling and isotropic chemical shift for the third aluminate hydrate

An unambiguous identification of an aluminate species by ^{27}Al MAS NMR requires a preknowledge of the isotropic chemical shift (δ_{iso}) and at least the quadrupolar product parameter ($P_Q = C_Q\sqrt{1+\eta_Q^2/3}$), which governs the degree of second-order quadrupolar shift of the center of gravity (δ^{cg}) for the resonance at a particular magnetic field. Even at a low magnetic field (7.05 T) the centerband from the TAH species does not exhibit a well-defined second-order quadrupolar lineshape but an asymmetric lineshape with a tail to low frequency. This is a characteristic feature for a small distribution in quadrupole coupling parameters [2] which shows that the Al resonance originates from an amorphous material or a disordered crystalline phase. Furthermore, the asymmetric lineshape prevents a direct determination of the quadrupole coupling parameters (C_Q and η_Q) from lineshape simulations of the central transition. Thus, δ_{iso} and P_Q are determined from the center of gravity of the central transition ($\delta^{cg}_{1/2,-1/2}$), observed at four magnetic fields (7.05, 9.39, 14.09, and 21.15 T), using the relationship [21]

$$\delta^{cg}_{1/2,-1/2} = \delta_{iso} - P_Q^2 \frac{C_{1/2,-1/2}}{\nu_L^2}$$
$$C_{1/2,-1/2} = \frac{3}{40}\frac{I(I+1)-3/4}{I^2(2I-1)^2} \quad (1)$$

where $I=5/2$ for ^{27}Al. Fig. 2 illustrates $\delta^{cg}_{1/2,-1/2}$ as a function of $C_{1/2,-1/2}/\nu_L^2$ for the TAH species in *C1_H* hydrated for 12 weeks, observed at the four different ^{27}Al Larmor frequencies (ν_L=78.16, 104.18, 156.32, and 234.52 MHz). Least-squares analysis to the data in Fig. 2 gives $\delta_{iso}=5.0\pm0.1$ ppm and $P_Q = C_Q\sqrt{1+\eta_Q^2/3} = 1.20\pm0.10$ MHz, where the latter correspond to a quadrupole coupling constant of $C_Q=1.13\pm0.18$ MHz. The small C_Q value indicates that the AlO_6 octahedron in TAH is highly symmetric. Moreover, we note that P_Q is larger than the value reported for ettringite [12] but slightly smaller than the P_Q values reported for the AFm phases monosulphate [12], $Ca_2[Al(OH)_6]OH{\cdot}6H_2O$ [12], and Friedels salt [20].

3.3. Characterization of the third aluminate hydrate by $^{27}Al\{^1H\}$ CP/MAS NMR

To investigate the local environment of the Al^{3+} ion in TAH, the *C1_H* sample hydrated for 12 weeks is studied by ^{27}Al{^{1}H} CP/MAS NMR. This sample is chosen because ettringite, monosulphate, and TAH are all clearly observed in the single-pulse ^{27}Al MAS spectrum (Fig. 3a). The ^{27}Al{^{1}H} CP/MAS NMR spectrum, shown in Fig. 3b, exhibits resonances from ettringite, monosulphate, and the TAH phase. To verify that these resonances are a result of ^{1}H→^{27}Al magnetization transfer, a "null experiment" is also performed (Fig. 3c), where the initial 90° ^{1}H pulse of the CP sequence is omitted. The absence of resonances in this spectrum confirms that the phase cycle of the CP experiment cancels any build-up of magnetization from the long ^{27}Al contact-time pulse. Thus, the ^{27}Al{^{1}H} CP/MAS NMR spectrum (Fig. 3b) demonstrates that ^{1}H atoms are present in close proximity to the Al site in the TAH species. The

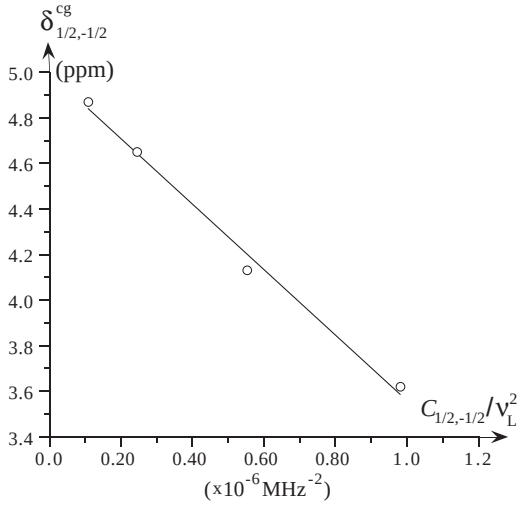

Fig. 2. Plot of the center of gravity ($\delta^{cg}_{1/2,-1/2}$) for the ^{27}Al central transition for the TAH species in *C1_H* (hydrated for 12 weeks) observed at four magnetic field strength (7.05, 9.39, 14.09 and 21.15 T) as a function of the parameter $C_{1/2,-1/2}/\nu_L^2$ (c.f., Eq (1)). The line corresponds to the result of linear regression analysis of the data, which gives the δ_{iso} and P_Q parameters for ^{27}Al in TAH (see text).

relative enhancement of the resonances from monosulphate and TAH relative to the peak from ettringite (Fig. 3b) reflect the fact that the Hartmann-Hahn matching condition for a quadrupole nucleus depends on the magnitude of the quadrupole splitting ($\nu_Q = \frac{3}{20}C_Q$ for ^{27}Al), the rf field strengths ($\nu_{rf}(^{27}Al)$ and $\nu_{rf}(^1H)$), and the spinning frequency (ν_R) [22,23]. For CP from ^{1}H to the ^{27}Al central transition the Hartmann-Hahn matching condition is [24]:

$$\nu_{rf}(^1H) = \nu_{rf}(^{27}Al) \quad \text{for} \quad \nu_Q \ll \nu_{rf}(^{27}Al) \tag{2}$$

$$\nu_{rf}(^1H) = 3\nu_{rf}(^{27}Al) \quad \text{for} \quad \nu_Q \gg \nu_{rf}(^{27}Al) \tag{3}$$

while the matching condition is not well defined in the intermediate range $\nu_Q \approx \nu_{rf}(^{27}Al)$ [23]. For strong quadrupole couplings (Eq. (3)), the parameter $\alpha=[\nu_{rf}(^{27}Al)]^2/(\nu_Q\nu_R)$ also needs consideration, since Eq. (3) holds for $\alpha \gg 1$ (slow-speed spinning) while the Hartmann-Hahn condition must fulfill one of the sideband conditions $\nu_{rf}(^1H)=3\nu_{rf}(^{27}Al)\pm n\nu_R$ ($n=1, 2$) for $\alpha \ll 1$ (high-speed spinning) [23]. The CP dynamics are investigated by ^{27}Al{^{1}H} CP/MAS NMR in Fig. 4a, which displays the intensity of the centerbands for ettringite, monosulphate, and TAH observed for an array of ^{27}Al rf field strengths ($\nu_{rf}(^{27}Al)=\gamma_{Al}B_{1Al}/2\pi=18-57$ kHz) and a constant ^{1}H rf field strength ($\nu_{rf}(^1H)=\gamma_H B_{2H}/2\pi=56$ kHz). In contrast to cross-polarization from ^{1}H to a spin $I=1/2$ nucleus (e.g., ^{13}C, ^{29}Si), the curves in Fig. 4a show that ^{1}H polarization is transferred to ^{27}Al for a range of ^{27}Al rf field strengths and not only at the Hartmann-Hahn matching condition (Eqs. (2) and (3)). For ettringite the maximum transfer of magnetization from ^{1}H to the ^{27}Al central transition is observed at the highest $\nu_{rf}(^{27}Al)$ field strength, in agreement with the matching condition $\nu_{rf}(^1H)\approx\nu_{rf}(^{27}Al)$ for a quadrupole nucleus experiencing a very small quadrupole coupling (Eq. (2)). The magnetization transfers for monosulphate and TAH as a function of $\nu_{rf}(^{27}Al)$ are very similar (Fig. 4a) and exhibit maxima at $\nu_{rf}(^1H)\approx3\nu_{rf}(^{27}Al)$ and $\nu_{rf}(^1H)\approx\nu_{rf}(^{27}Al)$ for both phases. This may reflect the fact that these phases possess quadrupole splittings, ν_Q=255 kHz (monosulphate [12]) and ν_Q=180 kHz (TAH, *vide supra*), which correspond to the intermediate range where the Hartmann-Hahn match is not well-defined.

Further information about the ^{1}H atoms in the ^{27}Al coordination sphere of the TAH species may be achieved from the cross-relaxation rate (T_{AlH}) and rotating-frame relaxation times ($T^{Al}_{1\rho}$ and $T^{H}_{1\rho}$) which describes the build-up and decay of cross-polarized signal intensity. This is due to the fact that the magnetization transfer is governed by ^{1}H-^{27}Al dipolar couplings (D_{Al-H}) which are inversely proportional to the cube of the H-Al distances ($D_{Al-H}\propto 1/r^3_{AlH}$). The build-up and decay of cross-polarized magnetization ($M_x(t)$) as a function of the contact time ($t=\tau_{CP}$) is given by

$$M_x(t) = \frac{M^H(0)}{\lambda}\exp\left(-t/T^H_{1\rho}\right)[1-\exp(-\lambda t/T_{AlH})] \tag{4}$$

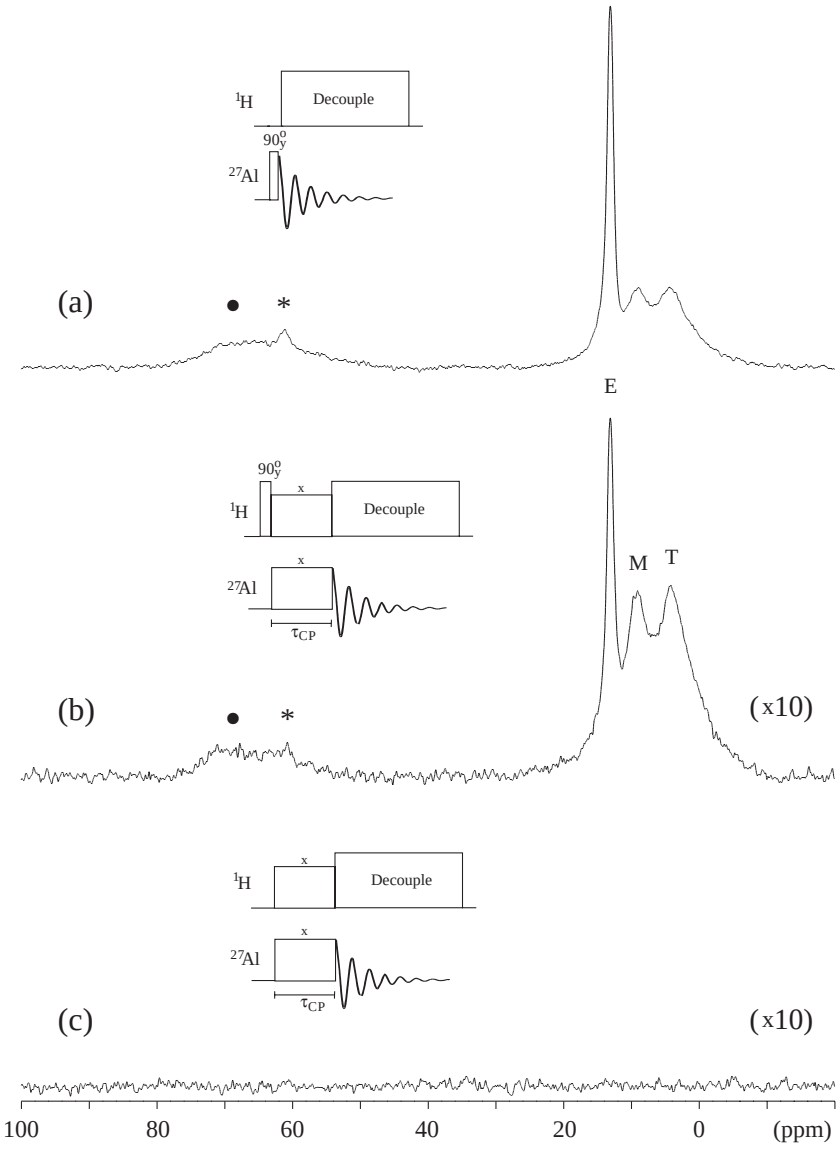

Fig. 3. ^{27}Al MAS and CP/MAS NMR spectra (9.39 T, ν_R=5.0 kHz) of *C1_H* hydrated for 12 weeks. (a) Standard ^{27}Al MAS NMR spectrum obtained with high-power ^{1}H decoupling. (b) ^{27}Al{^{1}H} CP/MAS NMR spectrum employing a CP contact time of τ_{CP}=0.2 ms, and the rf field strengths ν_{rf}(^{27}Al)=18 kHz, ν_{rf}(^{1}H)=56 kHz. (c) A "null-experiment" using the same experimental conditions as in part (b) except for the initial 90° ^{1}H pulse, which is omitted from the pulse sequence (see insets). The asterisks (*) indicate spinning sidebands from ettringite, while the filled circle (●) indicates the centerband for tetrahedrally coordinated Al in the C-S-H phase. The centerbands from ettringite, monosulphate, and the TAH species are denoted by E, M, and T, respectively. A vertical expansion by a factor of 10 is employed for the spectra in (b) and (c) as compared to the spectrum in (a).

where $\lambda = 1+(T_{AlH}/T^{Al}_{1\rho})-(T_{AlH}/T^{H}_{1\rho})$ and $M^H(0)$ is the ^{1}H magnetization after the initial 90°_y ^{1}H pulse [25]. This relationship holds for ^{1}H→ ^{27}Al cross polarization [26] for the spin systems studied and the present experimental conditions. However, the $T^{Al}_{1\rho}$ and $T^{H}_{1\rho}$ relaxation times cannot be determined independently from a fit of Eq. (4) to the variation in $M_x(t)$ as a function of τ_{CP} observed in CP contact-time experiments. Thus, the $T^{Al}_{1\rho}$ values are determined from separate ^{27}Al spin-lock experiments, employing the same rf pulse sequence and approach as in an earlier ^{29}Si{^{1}H} CP/MAS NMR study of thaumasite [27]. The ^{27}Al sites in ettringite, monosulphate, and TAH are studied by variable contact-time ^{27}Al{^{1}H} CP/MAS NMR experiments for the *C1_H* sample hydrated for 1 year. These experiments employ ^{27}Al rf field strengths of 17 kHz for monosulphate and TAH and ν_{rf}(^{27}Al)=53 kHz for ettringite and a fixed ^{1}H field of ν_{rf}(^{1}H)=56 kHz. Deconvolution of these spectra gives the signal intensities as a function of τ_{CP} shown in Fig. 4b for ettringite, monosulphate, and TAH. The curves correspond to the results from least-squares fits of Eq. (4) to the centerband intensities, employing the $T^{Al}_{1\rho}$ values, determined from ^{27}Al spin-lock experiments (Table 3), as a fixed parameter in the individual fits. The fits give the T_{AlH} and $T^{H}_{1\rho}$ values listed in Table 3 for ettringite, monosulphate, and TAH in the *C1_H* sample hydrated for 1 year. For comparison, the cross-relaxation and rotating-frame relaxation times are also determined for a synthetic sample of ettringite (Table 3). These values are observed to be very similar to those observed

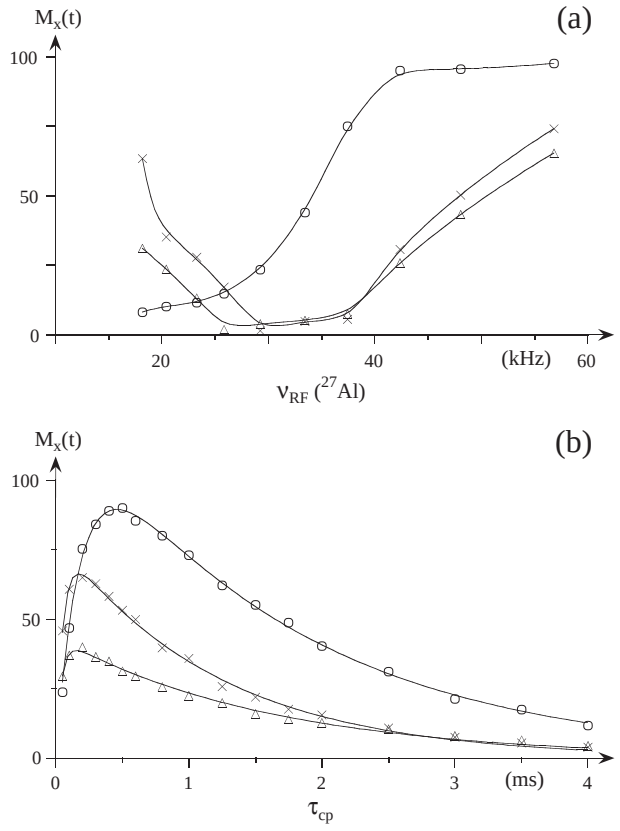

Fig. 4. (a) The variation in ^{27}Al centerband intensity in ^{27}Al{^{1}H} CP/MAS NMR experiments (9.39 T, ν_R=5.0 kHz, τ_{CP}=0.4 ms) as a function of the ^{27}Al rf field strength (ν_{rf}(^{27}Al)) for a fixed ^{1}H rf field (ν_{rf}(^{1}H)=56 kHz) for ettringite, monosulphate, and TAH in *C1_H* hydrated for 12 weeks. (b) The variation in ^{27}Al magnetization as a function of the contact time (τ_{CP}) in ^{27}Al{^{1}H} CP/MAS NMR spectra of *C1_H* hydrated for 1 year. The experiments employed ν_{rf}(^{27}Al)=16 kHz for monosulphate and TAH, ν_{rf}(^{27}Al)=57 kHz for ettringite, and ν_{rf}(^{1}H)=56 kHz for all three phases. The curves show the results from least-squares fitting of the data to Eq. (4) (see text). Open circles (○), ettringite; open triangles (△), monosulphate; crosses (×), the TAH species.

for ettringite in the *C1_H* sample. The $T_{1\rho}^{Al}$ value for ettringite is more than two orders of magnitude greater than $T_{1\rho}^{Al}$ for monosulphate and TAH. This difference is ascribed to the smaller quadrupole coupling for ettringite as compared to the two other phases. More interestingly, the T_{AlH} and $T_{1\rho}^{H}$ values are of the same order of magnitude for the three phases studied. This demonstrates that the Al–H environments in these phases are similar. From single-crystal XRD studies of ettringite [28] and monosulphate [29], it is known that Al is octahedrally coordinated to six OH^- groups, however, the positions of the H atoms were not reported in either of these investigations. The $Al(OH)_6^{3-}$ coordination is also observed for Al in Friedels salt, for which the atomic H positions have been reported [30]. Examination of the $Al(OH)_6^{3-}$ unit in the low-temperature α-form of Friedels salt [20,30] shows Al–H distances in the range 2.5–2.6Å. Obviously, Al–H distances in a similar range are expected for the $Al(OH)_6^{3-}$ groups in ettringite and monosulphate which may justify the small values observed for the T_{AlH} cross-relaxation time for these two phases. Since significantly longer Al–H distances would result in longer T_{AlH} values, the similarity of the T_{AlH} value observed for TAH with those for ettringite and monosulphate strongly indicates that the local Al–H environment in TAH is very similar to the octahedrally coordinated Al environment ($Al(OH)_6^{3-}$) in ettringite and monosulphate. Thus, the observation of the TAH species by ^{27}Al{^{1}H} CP/MAS NMR (Fig. 3b) and the close similarity in ^{27}Al{^{1}H} CP behaviour for TAH and monosulphate, strongly suggests that OH^- groups are directly bonded to aluminium in the TAH phase, most likely in the form of $Al(OH)_6^{3-}$ or at least as $O_xAl(OH)_{6-x}^{(3+x)-}$ octahedra.

3.4. Formation of the third aluminate hydrate during Portland cement hydration

The formation of the aluminium-containing hydration products have been followed by quantitative ^{27}Al MAS NMR for *C1_H* from 6 h to 30 weeks of hydration. Fig. 5a illustrates the equivalent quantities of Al_2O_3 (wt.%) in ettringite, monosulphate, and of tetrahedrally coordinated aluminium (Al_{IV}) incorporated in the chain structure of silicate tetrahedra of the C-S-H phase. The evolution with time for ettringite shows that the largest quantity of this phase occurs after hydration for 1 day, in agreement with earlier ^{27}Al MAS NMR studies of Portland cement hydration [31]. The subsequent decrease in the amount of ettringite is accompanied by an increase in the quantity of monosulphate, which slowly increases with increasing hydration time for the time of hydration studied. After 30 weeks of hydration the equivalent quantities of Al_2O_3 in these phases are 0.21±0.05 wt.% (ettringite) and 0.25±0.05 wt.% (monosulphate), which correspond to 2.6 wt.% ettringite ($Ca_6[Al(OH)_6]_2(SO_4)_3{\cdot}26H_2O$) and 1.5 wt.% monosulphate ($Ca_4[Al(OH)_6]_2SO_4{\cdot}6H_2O$), assuming stoichiometric compositions for these phases. Fig. 5b shows the sum of Al_2O_3 in ettringite and monosulphate and the equivalent quantity of Al_2O_3 in TAH. The decrease of Al_2O_3 in ettringite and monosulphate from 1 to 4 days of hydration suggests that the amount of aluminium, released by this decrease, contributes to the formation of the TAH species. However, the Al_2O_3 content in ettringite and

Table 3
Time constants for the ^{1}H-^{27}Al cross-relaxation (T_{A1H}) and the ^{1}H and ^{27}Al rotation-frame relaxation ($T_{1\rho}^{H}$ and $T_{1\rho}^{Al}$) determined from ^{27}Al{^{1}H} CP/MAS experiments for ettringite, monosulphate, and the third aluminate hydrate (TAH) for *C1_H* hydrated for 1 year and for a synthetic sample of ettringite

Phase	T_{A1H} (ms)[a]	$T_{1\rho}^{H}$ (ms)[a]	$T_{1\rho}^{Al}$ (ms)[b]
Synthetic ettringite	0.202±0.005	2.11±0.02	11.7±0.3
Ettringite	0.188±0.007	1.71±0.05	10.4±0.3
Monosulphate	0.09±0.02	1.61±0.05	0.072±0.005
TAH	0.19±0.03	1.19±0.03	0.076±0.005

[a] Parameters determined from a fit of Eq. (4) to the signal intensities observed in variable contact-time ^{27}Al{^{1}H} CP/MAS experiments (Fig. 4b).
[b] Values obtained from ^{27}Al spin-lock CP/MAS experiments using the approach in Ref. [27].

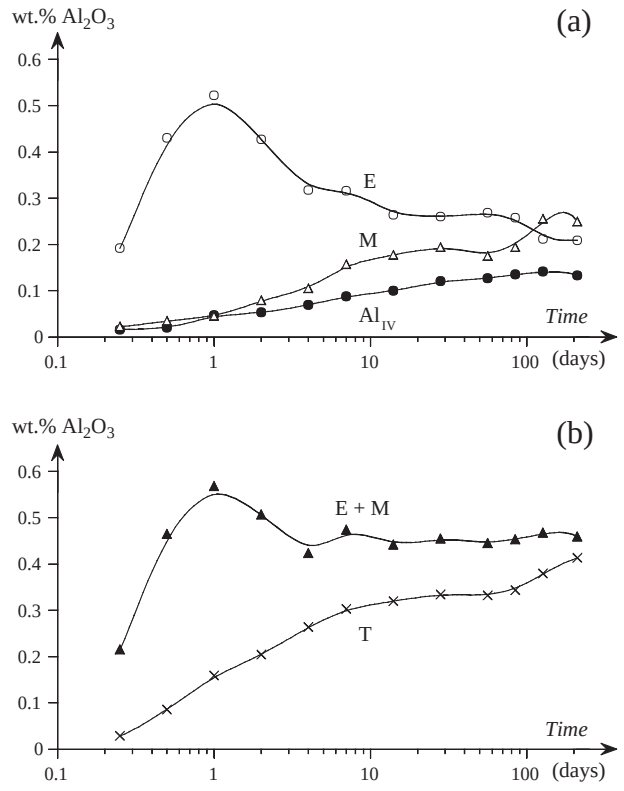

Fig. 5. Graphs illustrating the equivalent quantities of Al_2O_3 (wt.%) in ettringite, monosulphate, TAH, and Al_{IV} in the C-S-H phase following the hydration of *C1_H* and determined from ^{27}Al MAS NMR. Part (a): open circles (○), ettringite; open triangles (△), monosulphate; filled circles (●), Al_{IV} in the C-S-H phase. Part (b): filled triangles (▲), the sum of Al_2O_3 in ettringite and monosulphate; crosses (×), Al_2O_3 in the TAH species.

monosulphate is almost invariant from 4 days to 30 weeks of hydration, while the quantity of Al_2O_3 in TAH slowly increases during this period of time. This demonstrates that TAH is not only formed at the expense of ettringite but also from another source of Al in the hydrating cement. This source is most likely Al^{3+} ions incorporated in alite and belite, which are released during the prolonged hydration of these phases. After 30 weeks of hydration the equivalent quantity of Al_2O_3 is 0.41±0.05 wt.% in TAH, which is about three times higher than the value (0.13±0.02 wt.%) for Al_{IV} incorporated in the C-S-H phase (Fig. 5a). Deconvolution of the ^{29}Si MAS NMR spectrum of *C1_H* hydrated for 30 weeks (not shown) gives the ratio $Al_{IV}/Si=0.045$ for the C-S-H phase, which is somewhat smaller than the ratios Al/Si=0.095–0.129 determined by energy dispersive X-ray spectroscopy (EDS) microanalysis for the C-S-H in mortars prepared from an ordinary Portland cement and hydrated for 28 and 300 days [32]. However, the EDS method does not distinguish between Al in tetrahedral and octahedral (Al_{VI}) coordination. Thus, if the TAH species actually is octahedrally coordinated Al incorporated in the C-S-H structure, the ^{27}Al and ^{29}Si MAS NMR analyses would result in the ratio $(Al_{IV}+Al_{VI})/Si=0.187$ for the C-S-H in *C1_H* hydrated for 30 weeks. This ratio is significantly larger than the ratios determined by EDS/SEM for an ordinary Portland cement with a higher bulk Al_2O_3 content (2.2 wt.% Al_2O_3 [32]), which strongly suggests that the ^{27}Al resonance at $\delta_{iso}=5.0$ ppm does not originate from octahedrally coordinated Al in the C-S-H phase. Furthermore, the combination of ^{29}Si MAS NMR and EDS/TEM by Richardson and Lowe in a very recent study of the C-S-H formed in a white Portland cement (Aalborg Portland) activated with 5 M KOH shows that Al_{IV} incorporated in the silicate chain structure (^{29}Si NMR) accounts for the total quantity of Al in the C-S-H as observed by EDS/TEM [33]. In that work both ^{29}Si MAS NMR and EDS/TEM give Al/Si ratios around 0.06 for the C-S-H [33] which is very similar to the Al_{IV}/Si ratio determined by ^{29}Si MAS NMR for the C-S-H phase in *C1_H* hydrated for 30 weeks. We note that the quantitative ^{27}Al MAS NMR analysis of *C1_H* hydrated for 30 weeks gives the sum of 1.05±0.10 wt.% Al_2O_3 for ettringite, monosulphate, TAH, the penta-coordinated Al site (0.05±0.01 wt.% Al_2O_3), and Al_{IV} incorporated in the C-S-H phase, which may be compared to the total Al_2O_3 content (1.16±0.05 wt.%) in the sample. The remaining part of Al_2O_3 (<0.26 wt.%), which is not observed by ^{27}Al MAS NMR, is expected mainly to be present in phases resulting from hydration of the ferrite phase, where the strong nuclear-electron dipolar couplings between ^{27}Al and the unpaired electrons of Fe^{3+} prevents observation of Al atoms in the close proximity to Fe^{3+} ions.

3.5. Effects of sulphate ions on the formation of the third aluminate hydrate

To further investigate the formation of TAH, the hydration series of white Portland cement and white Portland clinkers containing additional quantities of gypsum (c.f., Table 2) have been studied by ^{27}Al MAS NMR. Fig. 6 illustrates ^{27}Al MAS NMR spectra of the samples hydrated for 8 weeks for these series. These spectra clearly reveal that the quantity of added gypsum affects the hydration products containing Al in octahedral coordination. For the white Portland cement (Fig. 6a–c), it is observed that the ettringite to monosulphate ratio increases with an increasing amount of added gypsum to the cement paste. Thus, the increased quantity of sulphate ions stabilizes the sulphate-rich ettringite phase and prevents its transformation into monosulphate with a lower SO_4^{2-} content. From the ^{27}Al MAS NMR spectra (Fig. 6a–c) it is also apparent that the quantity of TAH decreases with increasing gypsum content. This supports the finding in the previous section that Al^{3+} ions, released by the decomposition of ettringite, contribute to the formation of the TAH species. Alternatively, Al^{3+} ions released from other sources (e.g., alite and belite) may form ettringite due to the excess of sulphate ions, thereby preventing formation of TAH from these ions. The ^{27}Al MAS NMR spectrum of the white Portland clinker (*CL5_H*, Fig. 6d) exhibits no resonance from ettringite as a result of the very low SO_3 content (0.17 wt.%) in the

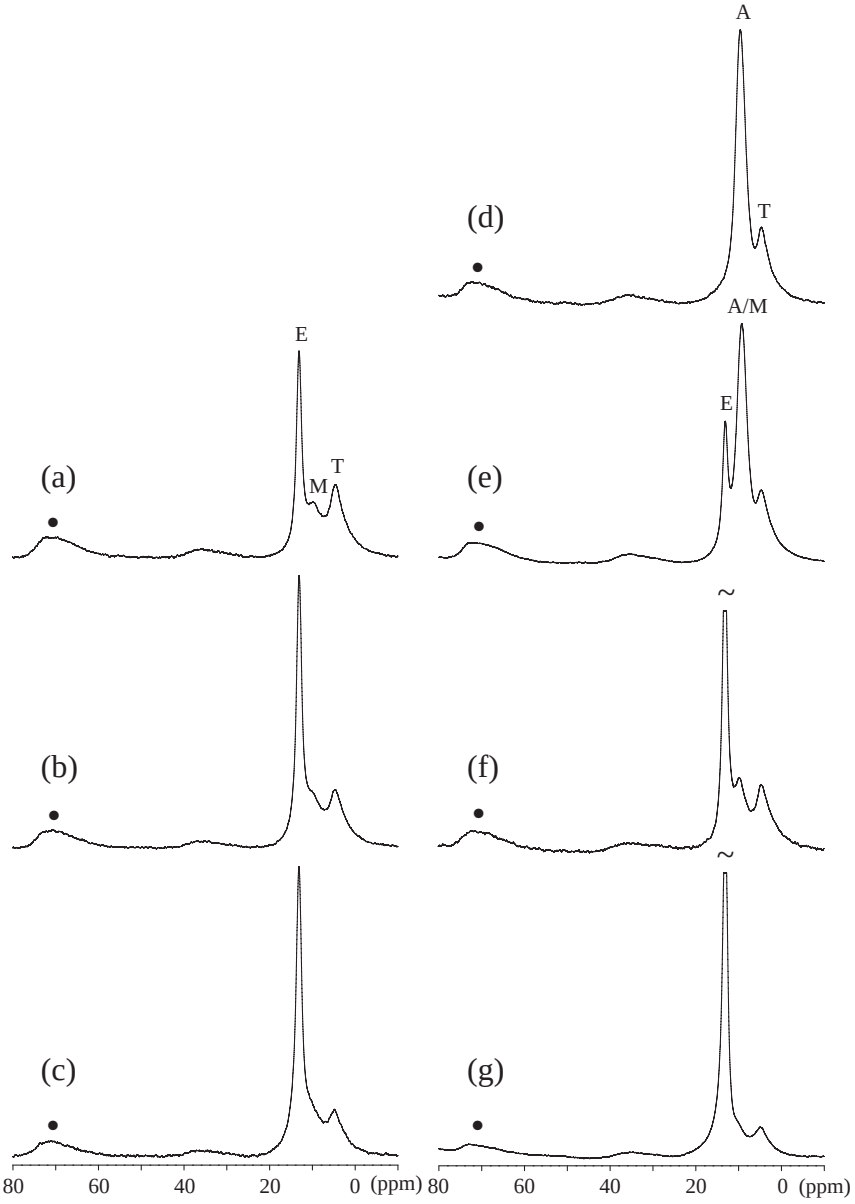

Fig. 6. ^{27}Al MAS NMR spectra (14.1 T, ν_R=13.0 kHz) obtained with high-power ^{1}H decoupling of the central transition after 8 weeks of hydration for (a) *C1_H*, (b) *C2_2G*, (c) *C3_5G*, (d) *CL5_H*, (e) *CL6_2G*, (f) *CL7_5G*, and (g) *CL8_10G*. The filled circle (●) indicates the centerband for Al_{IV} incorporated in the C-S-H phase while the centerbands from the hydration products ettringite, monosulphate, an AFm calcium aluminate hydrate, and the TAH species are denoted by E, M, A, and T, respectively. The spectra are shown on identical vertical scales, however, the centerband from ettringite is cut-off at 4/5 of its total height in (f) and (g).

anhydrous clinkers. However, TAH is clearly observed in this paste, demonstrating that this phase does not include sulphate ions. The main resonance in the spectrum is observed at $\delta^{cg}_{1/2,-1/2} \approx 9.5$ ppm and assigned to an AFm calcium aluminate hydrate ($Ca_2[Al(OH)_6]OH{\cdot}xH_2O$, $x=0$, 2, 3, 6), resulting from hydration of calcium aluminate ($Ca_3Al_2O_6$). Addition of gypsum to the white Portland clinkers (Fig. 6e–g) reproduces well the results derived for the white Portland cement, since an increasing quantity of ettringite is observed with increasing addition of gypsum. An increasing amount of gypsum also results in a decrease in the quantity of the AFm calcium aluminate hydrate, which in these spectra cannot be distinguished from monosulphate. Furthermore, the intensity of the resonance from TAH is slightly reduced with increasing gypsum content in accordance with the Al^{3+} ions being consumed by ettringite formation at high concentrations of sulphate ions.

3.6. Thermal stability of the third aluminate hydrate

To investigate the thermal stability of TAH, samples of *C1_H* hydrated for 3 years and subsequently heated at ambient conditions at 70, 90 150, and 200 °C for 24 h have been studied by ^{27}Al and ^{29}Si MAS NMR (Fig. 7). The ^{27}Al

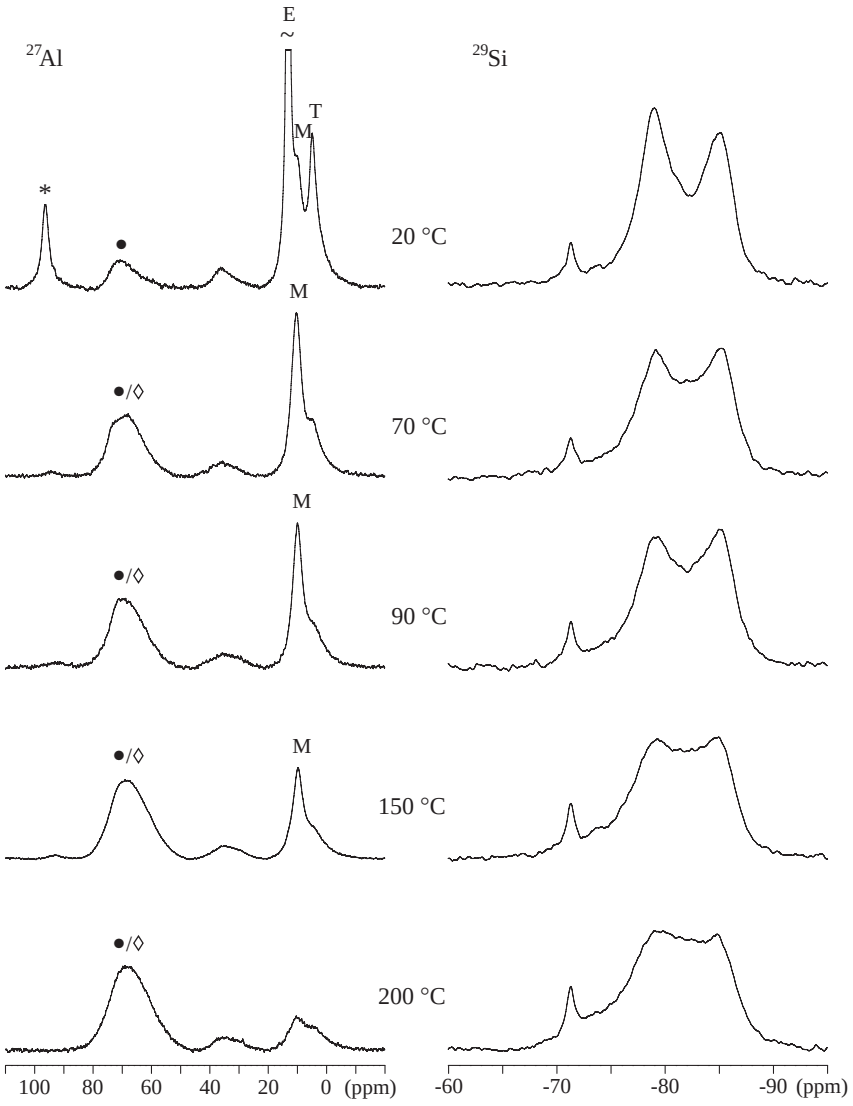

Fig. 7. ^{27}Al MAS NMR spectra (14.1 T, ν_R=13.0 kHz, high-power ^{1}H decoupling) and ^{29}Si MAS NMR spectra (9.4 T, ν_R=6 kHz) of wPc hydrated in water (*C1_H*) for 1080 days before heat treatment (20 °C) and after heating for 1 day at the temperatures 70, 90, 150, and 200 °C. The asterisk (*) indicates a spinning sideband from ettringite, the filled circle (●) the centerband for tetrahedral Al incorporated in the C-S-H phase, while the diamond (◊) indicates tetrahedral Al species originating from the decomposition of ettringite, monosulphate, and TAH. These hydrates are denoted by E, M, and T, respectively.

MAS NMR spectra demonstrate that the heat treatment significantly affects ettringite, monosulphate, and TAH. The spectrum of the *C1_H* sample heated at 70 °C shows that almost all ettringite and a major part of the TAH species have decomposed and formed monosulphate and an aluminate phase containing Al in tetrahedral coordination. The observed decomposition of ettringite to monosulphate after heat treatment at 70 °C is in accord with weight-loss measurements [1], Raman scattering and XRD studies of ettringite heated at ambient conditions [34], which indicate that the onset of the dehydration/decomposition of ettringite takes place at approx. 50 °C with a rapid loss of water. However, the thermal decomposition of ettringite has also been reported to occur at 114 °C from XRD and FTIR studies of a slurry of ettringite and water contained in a sealed capsule [35]. The increase in vapour pressure at elevated temperatures, caused by the use of a sealed capsule, may prevent the release of water at lower temperatures and thereby explain the higher decomposition temperature. This is in agreement with a recent weight-loss study of ettringite as a function of water pressure and temperature [36]. A significant decrease in intensity is also observed for TAH at 70 °C, demonstrating that this species decomposes at low temperature. The decomposition of TAH results in the formation of an amorphous aluminate phase containing Al in tetrahedral coordination, which has a centerband that cannot be resolved by ^{27}Al MAS NMR from the centerband for Al_{IV} incorporated in the C-S-H phase. The ^{29}Si MAS NMR spectra of the same samples (Fig. 7) show that the amount of Al_{IV} incorporated in the C-S-H phase, indirectly observed by the resonance from Q^2(1Al) SiO_4 species, does not increase when the temperature is raised to 70 and

90 °C. Thus, the increase in intensity for the Al_{IV} centerband at $\delta^{cg}_{1/2,-1/2} \approx 70$ ppm originates from the formation of a new Al_{IV} phase which, considering the width and featureless appearance of this resonance in the ^{27}Al MAS NMR spectra (Fig. 7), is amorphous. The quantity of this phase increases with increasing temperature and results also from the decomposition of monosulphate, which is observed in the temperature range 90–200 °C. The spectral region for Al_{VI} in the ^{27}Al MAS NMR spectrum of the sample heated to 200 °C includes two minor resonances ($\delta^{cg}_{1/2,-1/2} \approx 10$ ppm and $\delta^{cg}_{1/2,-1/2} \approx 5$ ppm), which are assigned to amorphous Al_{VI} species. These species are most likely also present at lower temperatures (90 and 150 °C) and subtraction of their resonances from the ^{27}Al MAS NMR spectra of the samples heated at 90 and 150 °C show that nearly all of the TAH species has decomposed at 90 °C. Examination of the ^{29}Si MAS NMR spectra for the temperatures 90–200 °C shows an increased degree of linebroadening of the Q^1, $Q^2(1Al)$, and Q^2 resonances from the C-S-H phase. In this temperature range, the C-S-H phase may loose some interlayer water molecules, resulting in a more rigid C-S-H structure which may explain the increased broadening of these resonances. Overall, the ^{29}Si MAS NMR spectra demonstrate that the calcium silicate layers of the C-S-H phase remain intact when the pastes are heated to 200 °C. This observation and the fact that TAH decomposes at temperatures below 90 °C strongly suggest that the $\delta_{iso} = 5.0$ ppm resonance in the ^{27}Al MAS NMR spectra does not originate from Al_{VI} incorporated in the C-S-H phase.

3.7. Formation of the third aluminate hydrate in C-S-H phases

A number of C-S-H phases have been prepared from $Ca(OH)_2$, SiO_2, and $NaAlO_2$ at a curing temperature of 20 °C, employing the initial molar ratio $(Al/Si)_i = 0.05$ and initial molar $(Ca/Si)_i$ ratios in the range 0.66–1.75. The Ca/Si ratio of 0.66 is the ideal ratio for a C-S-H with a dreierketten structure of SiO_4 tetrahedral chains on both sides of the CaO_2 principal layer and the absence of Ca^{2+} ions in the interlayer space, while Ca/Si = 0.83 is the ratio for the 11-Å and 14-Å tobermorites, $Ca_{4.5}Si_6O_{16}(OH)\cdot 5H_2O$ [37] and $Ca_5Si_6O_{16}(OH)_2\cdot 7H_2O$ [38], respectively (c.f., Fig. 8). Jennite ($Ca_9Si_6O_{18}(OH)_6\cdot 8H_2O$) [39] exhibits the ratio Ca/Si = 1.5. The largest value, $(Ca/Si)_i = 1.75$, corresponds to the ratio Ca/Si = 1.7–1.8 found for C-S-H in cement pastes [1]. The ^{27}Al MAS NMR spectra of the synthetic C-S-H samples (Fig. 9) demonstrate the absence of a resonance from TAH for the Ca/Si ratios $(Ca/Si)_i = 0.66$ and 0.75 for which Al is only present as Al_{IV} incorporated in the silicate chain structure. For the higher Ca/Si ratios the resonance from TAH is clearly observed and it is apparent that the quantity of this species is almost identical for the samples with $(Ca/Si)_i = 1.25$–1.75. The corresponding ^{29}Si MAS NMR spectra (not shown) clearly reveal that the $[Q^2 + Q^2(1Al)]/Q^1$ ratio decreases with increasing Ca/Si ratio and thereby also the average chain length of Si/Al_{IV} tetrahedra (CL). Thus, the C-S-H phases with a low Ca/Si ratio contain long average chains of SiO_4/AlO_4 tetrahedra (e.g., CL = 16.4 for $(Ca/Si)_i = 0.66$), while high Ca/Si ratios result in a C-S-H dominated by Q^1 units and thereby dimers of SiO_4 tetrahedra (e.g., CL = 2.6 for $(Ca/Si)_i = 1.75$). This observation is in full accord with earlier ^{29}Si MAS NMR studies of synthetic C-S-H phases with different Ca/Si ratios in the range $Ca/Si \approx 0.5$–2.0 [40,41]. The observation of TAH for $(Ca/Si)_i \geq 0.83$ indicates that the presence of Ca^{2+} ions in a significant concentration is required for the formation of this phase. However, two additional syntheses were performed, which employed the same recipe as for the $(Ca/Si)_i = 1.00$ sample but excluded either $Ca(OH)_2$ or SiO_2 from the synthesis mixture. The ^{27}Al MAS NMR spectra of these samples (not shown) show that TAH is not formed in either of the samples. This observation along with those for the samples with $0.66 < (Ca/Si)_i < 1.75$ suggest that TAH is only formed in the presence of a C-S-H phase. We note that powder-XRD studies of the C-S-H samples include only reflections which can be assigned to the C-S-H and small quantities of portlandite ($Ca(OH)_2$), the latter observed only for the samples with high $(Ca/Si)_i$ ratios. The absence of new reflections from TAH may be a sign of the amorphous/

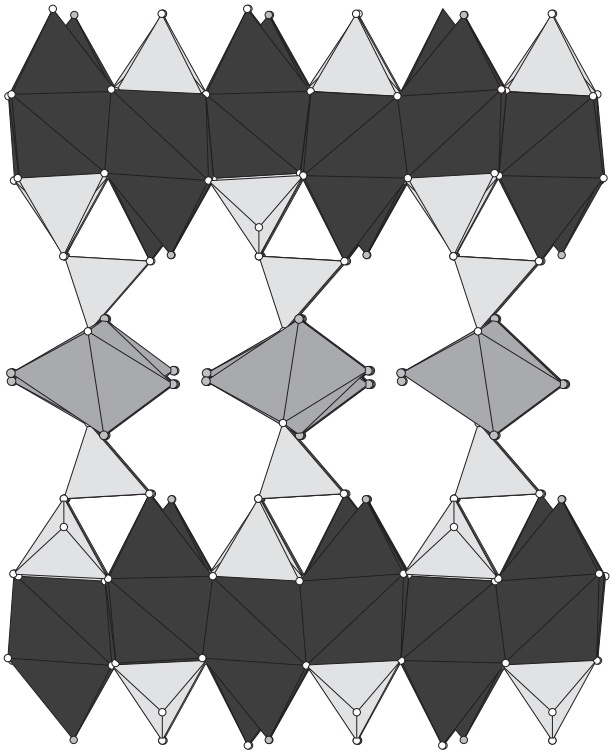

Fig. 8. Polyhedral model illustrating two principal layers of composition CaO_2 (dark polyhedra), surrounded by dreierketten of SiO_4 tetrahedral chains (light-grey tetrahedra) on both sides, and one interlayer containing octahedrally coordinated Ca^{2+} ions (grey polyhedra) and water molecules. The graphical representation is based on the most recent single-crystal XRD structure reported for 14-Å tobermorite [38] as seen along the [010] direction. The chains of SiO_4 tetrahedra are observed along the *b*-direction, i.e., perpendicular to the plane of the projection.

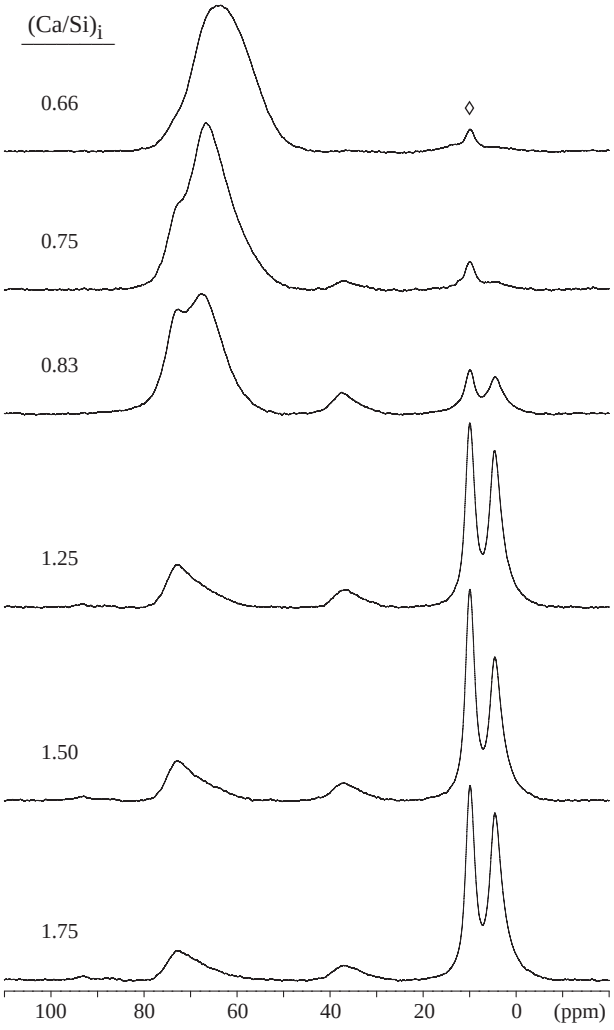

Fig. 9. ^{27}Al MAS NMR spectra (14.1 T, ν_R=13.0 kHz, high-power ^{1}H decoupling) of C-S-H phases synthesized with initial Ca/Si ratios in the range (Ca/Si)$_i$=0.66–1.75. The diamond illustrates the resonance ($\delta \approx 10$ ppm) from an impurity of a calcium aluminate hydrate ($CaAl_2O_4{\cdot}10H_2O$ and/or an AFm phase) which is observed for all Ca/Si ratios. The broadened resonance in the range 30–40 ppm originates from penta-coordinated Al. The individual spectra are shown on identical intensity scales, corrected for the actual sample weight used in the experiments.

disordered nature of this species combined with the presence of TAH in very small quantities. The decrease in average chain length of Si/Al$_{IV}$ tetrahedra with increasing Ca/Si ratio results in a C-S-H with a larger number of defects in the structure and on the C-S-H surface. This suggests that TAH may be formed either on the surface of the C-S-H or as a separate phase interstitified in the interlayer structure of the C-S-H. However, the latter hypothesis would result in a significant higher Al/Si ratio for the C-S-H, in contrast to EDS/SEM and EDS/TEM investigations of C-S-H phases [32,33]. This fact and the observation of the thermal decomposition of TAH at about 70–90 °C favours the suggestion of TAH being formed on the surface of the C-S-H grains, most likely physically adsorbed on the grain boundary of the C-S-H as a surface precipitate. Taylor has noted that the main layers in the C-S-H and AFm phases are oppositely charged which may produce strong mutual attractions that can physically destroy the AFm crystals [42]. Thus, the constituent layers of the AFm may be dispersed in the C-S-H, resulting in a poorly crystalline phase which cannot be detected by XRD or thermal methods. This proposal is compatible with the observations in the present study for the TAH species. Furthermore, the presence of such an AFm-type structure, which on the nanoscale is a separate phase, was incorporated in the general model for the C-S-H by Richardson and Groves [43] to account for trivalent cations (Al^{3+} and Fe^{3+}) in octahedral coordination. On the basis of these considerations, we propose that TAH is either a nanostructured amorphous/disordered aluminium hydroxide or a calcium aluminate hydrate produced in a less ordered form as a surface precipitate on the C-S-H phase.

3.8. The possibility of incorporation of octahedrally coordinated Al in the C-S-H structure

Faucon et al. have studied the incorporation of Al in C-S-H samples with different Ca/Si ratios [10]. For C-S-H phases with initial molar Ca/Si ratios in the range 1.0–1.7 they also observe a resonance at ~5 ppm (δ_{iso}=4.25 and P_Q=1.83 MHz [10]), which they assign to Al^{3+} substituting for Ca^{2+} ions in the principal layers of the C-S-H structure. It is well-known that the C-S-H exhibits diversity in both structure and composition depending on the Ca/Si ratio. Taylor distinguishes between C-S-H(I) and C-S-H(II) and proposes that these are structurally similar to 14-Å tobermorite (Ca/Si=0.83) and jennite (Ca/Si=1.5) [44]. Both of these phases as well as the 11-Å tobermorite contain a principal layer (with the composition CaO_2) of six- or seven-fold coordinated Ca^{2+} ions surrounded by SiO_4 tetrahedra on both sides (c.f., Fig. 8). The refined crystal structures for these crystalline calcium silicate hydrates have recently been reported and examination of the CaO_6 and CaO_7 polyhedra in the principal layers of these structures gives Ca–O bond lengths in the ranges: d_{Ca-O}=2.35–2.63Å (11-Å tobermorite, CaO_7 [37]); d_{Ca-O}=2.29–2.74Å (14-Å tobermorite, CaO_7 [38]); and d_{Ca-O}=2.33–2.54Å (jennite, CaO_6 [39]). These bond distances are significantly longer than those observed for AlO_6 octahedra in aluminate and calcium aluminate hydrates ($d_{Al-O} \approx 1.80$–1.95Å), which strongly suggests that Al^{3+} for Ca^{2+} substitution is not possible, since it would entail excessively long Al–O bonds. Moreover, the principal layers of the C-S-H structure are thermally stable to temperatures well above 300 °C and thus, it is unlikely that an Al$_{VI}$ site, obtained by substitution for Ca^{2+} ions, would decompose to Al$_{IV}$ by thermal treatment at 70–90 °C, as observed for the TAH species.

3.9. Penta-coordinated Al in the C-S-H structure

The ^{27}Al MAS NMR spectra of the hydrated white Portland cements (Figs. 1 and 6) and the C-S-H samples

(Fig. 9) include a low-intensity resonance from penta-coordinated Al ($\delta^{cg}_{1/2,-1/2} \approx 35$ ppm at 14.1 T). This resonance has also been observed in recent ^{27}Al MAS NMR studies of similar materials, from which the following ^{27}Al NMR parameters have been reported $\delta_{iso}=39.9\pm0.3$ ppm, $P_Q=5.1\pm0.2$ MHz (wPc [6]) and $\delta_{iso}=38.8$ ppm, $P_Q=3.2\pm0.2$ MHz (C-S-H [10]). Faucon et al. have tentatively assigned this resonance to Al^{3+} substituting for Ca^{2+} ions in the interlayers of the C-S-H [10]. The ^{27}Al MAS NMR spectra in Fig. 7 demonstrate that the resonance originates from an Al site which is stable upon heating to 200 °C. This thermal stability would be expected for an Al site in the C-S-H structure. The interlayer Ca^{2+} ions are seven-fold coordinated in 11-Å tobermorite [37] and octahedrally coordinated in 14-Å tobermorite [38] and jennite [39], where these sites exhibit Ca–O bond lengths in the ranges d_{Ca-O}(11-Å)=2.24–2.89 Å, d_{Ca-O}(14-Å)=2.26–2.69 Å, and d_{Ca-O}(jen)=2.33–2.77 Å. Obviously, the formation of a penta-coordinated Al site by substitution for interlayer Ca^{2+} ions requires a reduction in coordination environment by one or two oxygen atoms and that the cation-oxygen bond lengths are reduced to typical Al–O bond lengths in the range $d_{Al-O} \approx 1.80-1.95$ Å. The presence of such an Al site may be justified by examination of the local structure of the interlayer Ca^{2+} ions in 11-Å tobermorite. Fig. 10a illustrates the local environment of the interlayer Ca^{2+} ion in this mineral, based on the most recent XRD structure refinement [37], and shows that the Ca^{2+} ion is bonded to the oxygens of three interlayer water molecules and four oxygen atoms that are part of the chains of silicate tetrahedra. The water molecules are moderately flexible indicating that Al–O bond lengths less than 2.0Å can be achieved by displacement of these units. On the other hand, the oxygens of the silicate chains are part of a rigid structure, implying that these atoms hardly can be displaced in order to obtain Al–O bond lengths less than 2.0Å. Consideration of the geometry for the O1, O2, O6, and O7 atoms (Fig. 10a) shows that $d_{Al-O}<2.0$Å can be achieved only if the Al^{3+} ion is coordinated to two of these four oxygens, i.e., (O2, O1), (O2, O6) or (O2, O7). Of these combinations the coordination of the cation to O2 and O6 seems most plausible, considering the fact that these two oxygens exhibit the shortest Ca–O bond lengths of the CaO_7 unit. Moreover, the Ca–O1 and Ca–O7 bonds ($d_{Ca-O1}=d_{Ca-O7}=2.89$ Å) are significantly longer than the other five bonds ($d_{Ca-O}=2.24-2.41$Å) and these two bonds are oriented in the same direction as the shortest Ca–O2 bond, the bond angles being <(O2–Ca–O7)=58.0° and <(O2–Ca–O1)=56.8°. This suggests that the effects from the O1 and O7 oxygen atoms on the cation are shielded by the O2 atom, resulting in an effective coordination environment which is close to a penta-coordinated site. This "effective" coordination environment, illustrated in Fig. 10b, may justify the observation of an ^{27}Al NMR resonance in the spectral region for AlO_5 sites, which originates from Al^{3+} ions substituting for Ca^{2+} ions in the C-S-H interlayer. However, it cannot be excluded that a penta-coordinated Al site alternatively may arise from a defect site in the interlayer of the C-S-H structure.

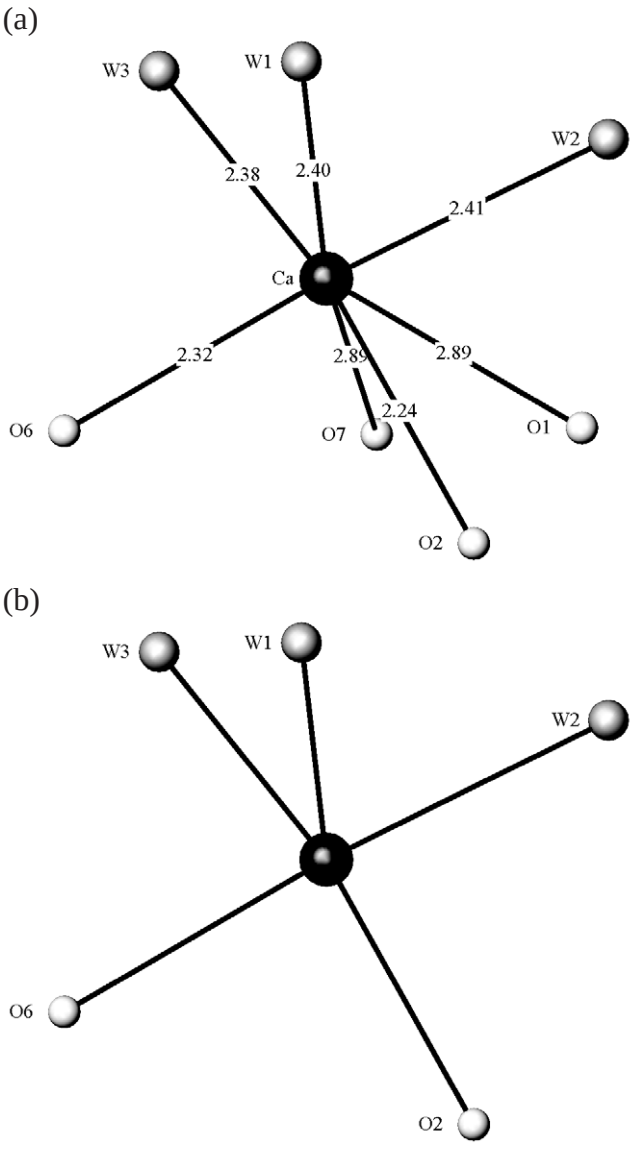

Fig. 10. (a) Structure of the CaO_7 unit in the interlayer of the 11-Å tobermorite obtained from data reported from single-crystal XRD [37]. W1, W2, and W3 are oxygen atoms of interlayer water molecules while O1, O2, O6, and O7 are oxygen atoms of the silicate chains. (b) Proposed local environment for the penta-coordinated Al site observed for C-S-H phases and ascribed to Al^{3+} ions substituting for interlayer Ca^{2+} ions.

4. Conclusions

^{27}Al MAS and ^{27}Al{^{1}H} CP/MAS NMR spectroscopies have been employed in the characterization of a new aluminate hydrate produced in hydrated Portland cements in addition to the AFt and AFm phases ettringite and monosulphate. This species is denoted the third aluminate

hydrate (TAH), and its formation and thermal stability have been investigated for a number of different white Portland cement mixtures and C-S-H samples. From these experiments the following can be summarized about the TAH species.

- ^{27}Al MAS NMR spectra, recorded at different magnetic fields, have demonstrated that TAH is an amorphous or disordered species and that the Al_{VI} site exhibits the isotropic chemical shift $\delta_{iso}=5.0$ ppm and the quadrupole product parameter $P_Q=1.2$ MHz.
- The ^{27}Al{^{1}H} CP/MAS NMR experiments have revealed that TAH contains an Al_{VI} site with hydrogen atoms in its nearest coordination sphere in the form of either $A1(OH)_6^{3-}$ or $O_xA1(OH)_{6-x}^{(3+x)}$ units.
- Quantitative ^{27}Al MAS NMR of hydrated white Portland cements has shown that the quantity of TAH increases with increasing hydration time and that it is most likely formed at the expense of ettringite, and from Al^{3+} ions incorporated in alite and belite, which are released during prolonged hydration of these phases. The equivalent quantity of Al_2O_3 in TAH is very low (0.41 wt.% for a white Portland cement hydrated for 30 weeks), which may justify that it has not been observed earlier by other techniques such as X-ray diffraction.
- The TAH phase does not contain sulphate ions, however, an increase in the quantity of sulphate ions in the hydrating cement reduces the quantity of produced TAH.
- The TAH species decomposes by thermal treatment at 70–90 °C and forms a new phase containing AlO_4 tetrahedra.
- The TAH species has been detected in C-S-H phases synthesized at room temperature when the Ca/Si ratio is above 0.83. For Ca/Si ratios in the range $(Ca/Si)_i=1.25$–1.75 the quantity of produced TAH is almost constant.
- Examination of the Ca–O bond lengths in the principal layers of the structures for 11-Å tobermorite, 14-Å tobermorite, and jennite has strongly suggested that TAH does not originate from Al^{3+} for Ca^{2+} substitution in these layers of the C-S-H.

From these observations it is proposed that TAH is an amorphous/disordered aluminium hydroxide or a calcium aluminate hydrate produced as a separate phase or as a nanostructured surface precipitate on the C-S-H phase.

Finally, it has been justified that the ^{27}Al resonance, observed for penta-coordinated Al in hydrated Portland cements and C-S-H phases, may originate from Al^{3+} ions substituting for Ca^{2+} ions in the interlayers of the C-S-H phase.

Acknowledgements

The use of the facilities at the Instrument Centre for Solid-State NMR Spectroscopy, University of Aarhus, sponsored by the Danish Natural Science Research Council, the Danish Technical Science Research Council, Teknologistyrelsen, Carlsbergfondet, and Direktør Ib Henriksens Fond, is acknowledged. We thank the two Danish Research Councils for financial support (J.nr. 2020-00-0018). Professor R. J. Kirkpatrick (University of Illinois at Urbana-Champaign), Dr. A. R. Brough and Dr. I. G. Richardson (University of Leeds), and Dr. E. Bonaccorsi (University of Pisa) are acknowledged for fruitful discussions related to this study.

References

[1] H.F.W. Taylor, Cement Chemistry, 2nd ed., Thomas Telford, London, 1997.
[2] J. Skibsted, H.J. Jakobsen, C. Hall, Direct observation of aluminum guest ions in the silicate phases of cement minerals by ^{27}Al MAS NMR spectroscopy, J. Chem. Soc., Faraday Trans. 90 (1994) 2095–2098.
[3] R. Fischer, H.J. Kuzel, Reinvestigation of the system $C_4A{\cdot}nH_2O$–$C_4A{\cdot}CO_2{\cdot}nH_2O$, Cem. Concr. Res. 12 (1982) 517–526.
[4] S. Komarneni, D.M. Roy, C.A. Fyfe, G.S. Kennedy, Naturally occurring 1.4 nm tobermorite and synthetic jennite: characterization by ^{27}Al and ^{29}Si MAS NMR spectroscopy and cation exchange properties, Cem. Concr. Res. 17 (1987) 891–895.
[5] I.G. Richardson, A.R. Brough, R. Brydson, G.W. Groves, C.M. Dobson, Location of aluminium in substituted calcium silicate hydrate (C-S-H) gels as determined by ^{29}Si and ^{27}Al and EELS, J. Am. Ceram. Soc. 76 (1993) 2285–2288.
[6] M.D. Andersen, H.J. Jakobsen, J. Skibsted, Incorporation of aluminum in the calcium silicate hydrate (C-S-H) of hydrated Portland cements: a high-field ^{27}Al and ^{29}Si MAS NMR investigation, Inorg. Chem. 42 (2003) 2280–2287.
[7] H. Stade, D. Müller, G. Scheler, ^{27}Al NMR spektroskopische untersuchungen zur koordination des Al in C-S-H (di, poly), Z. Anorg. Allg. Chem. 510 (1984) 16–24.
[8] H. Stade, D. Müller, On the coordination of Al in ill-crystallized calcium silicate hydrate (C-S-H) phases formed by hydration of tricalcium silicate and by precipitation reactions at ambient temperature, Cem. Concr. Res. 17 (1987) 553–561.
[9] D.S. Klimesch, A.S. Ray, Effect of quartz content on the nature of Al-substituted 11Å tobermorite in hydrothermally treated $CaO–Al_2O_3–SiO_2–H_2O$ systems, Adv. Cem. Res. 11 (1999) 179–187.
[10] P. Faucon, A. Delagrave, J.C. Petit, C. Richet, J.M. Marchand, H. Zanni, Aluminum incorporation in calcium silicate hydrates (C-S-H) depending on their Ca/Si ratio, J. Phys. Chem., B 103 (1999) 7796–7802.
[11] J. Hjorth, J. Skibsted, H.J. Jakobsen, ^{29}Si MAS NMR studies of Portland cement components and effects of microsilica on the hydration reaction, Cem. Concr. Res. 18 (1988) 789–798.
[12] J. Skibsted, E. Henderson, H.J. Jakobsen, Characterization of calcium aluminate phases in cements by ^{27}Al MAS NMR spectroscopy, Inorg. Chem. 32 (1993) 1013–1027.
[13] S. Kwan, J. LaRosa-Thompson, M.W. Grutzeck, Structures and phase relations of aluminum-substituted calcium silicate hydrate, J. Am. Ceram. Soc. 79 (1996) 967–971.
[14] P. Faucon, T. Charpentier, A. Nonat, J.C. Petit, Triple-quantum two-dimensional ^{27}Al magic angle nuclear magnetic resonance study of the aluminium incorporation in calcium silicate hydrates, J. Am. Chem. Soc. 120 (1998) 12075–12082.
[15] I.G. Richardson, A.R. Brough, G.W. Groves, C.M. Dobson, The characterization of hardened alkali-activated blast-furnace slag pastes and the nature of the calcium silicate hydrate (C-S-H) phase, Cem. Concr. Res. 24 (1994) 813–829.

[16] M.D. Andersen, H.J. Jakobsen, J. Skibsted, Characterization of white Portland cement hydration and the C-S-H structure in the presence of sodium aluminate by ^{27}Al and ^{29}Si MAS NMR spectroscopy, Cem. Concr. Res. 34 (2004) 857–868.
[17] H.J. Jakobsen, P. Daugaard, E. Hald, D. Rice, E. Kupce, P.D. Ellis, A 4-mm probe for ^{13}C CP/MAS NMR of solids at 21.15 T, J. Magn. Reson. 156 (2002) 152–154.
[18] J. Skibsted, N.C. Nielsen, H. Bildsøe, H.J. Jakobsen, Satellite transitions in MAS spectra of quadrupolar nuclei, J. Magn. Reson. 95 (1991) 88–117.
[19] P. Faucon, T. Charpentier, D. Bertrandie, A. Nonat, J. Virlet, J.C. Petit, Characterization of calcium aluminate hydrates and related hydrates of cement pastes by ^{27}Al MQ-MAS NMR, Inorg. Chem. 37 (1998) 3726–3733.
[20] M.D. Andersen, H.J. Jakobsen, J. Skibsted, Characterization of the α–β phase transition in Friedels salt ($Ca_2Al(OH)_6Cl{\cdot}H_2O$) by variable-temperature ^{27}Al MAS NMR spectroscopy, J. Phys. Chem., A 28 (2002) 6676–6682.
[21] A. Samoson, Satellite transition high-resolution NMR of quadrupolar nuclei in powders, Chem. Phys. Lett. 119 (1985) 29–32.
[22] A. Vega, MAS NMR spin locking of half-integer quadrupolar nuclei, J. Magn. Reson. 96 (1992) 50–68.
[23] A. Vega, CP/MAS of quadrupolar $S=3/2$ nuclei, Solid State Nucl. Magn. Reson. 1 (1992) 17–32.
[24] S.R. Hartmann, E.L. Hahn, Nuclear double resonance in the rotating frame, Phys. Rev. 128 (1962) 2042–2053.
[25] M. Mehring, Principles of High Resolution NMR in Solids, Springer-Verlag, Berlin, 1983.
[26] T.H. Walter, G.L. Turner, E. Oldfield, Oxygen-17 cross-polarization NMR spectroscopy of inorganic solids, J. Magn. Reson. 76 (1988) 106–120.
[27] J. Skibsted, L. Hjorth, H.J. Jakobsen, Quantification of thaumasite in cementitious materials by ^{29}Si{^{1}H} cross-polarization magic-angle spinning NMR spectroscopy, Adv. Cem. Res. 7 (1995) 69–83.
[28] A.E. Moore, H.F.W. Taylor, Crystal structure of ettringite, Acta Crystallogr., B 26 (1970) 386–393.
[29] R. Allmann, Refinement of the hybrid layer structure $[Ca_2Al(OH)_6]^{+}\cdot[(1/2)SO_4{\cdot}3H_2O]^{-}$, Neues Jahrb. Mineral., Monatsh. H3 (1977) 136–144.
[30] A. Terzis, S. Filippakis, H.-J. Kuzel, H. Burzlaff, The crystal structure of $Ca_2Al(OH)_6Cl{\cdot}2H_2O$, Z. Kristallogr. 181 (1987) 29–34.
[31] J. Skibsted, O.M. Jensen, H.J. Jakobsen, Hydration kinetics for the alite, belite, and calcium aluminate phase in Portland cements from ^{27}Al and ^{29}Si MAS NMR spectroscopy, Proc. 10th Int. Congr. Chem. Cem., Gothenburg, Sweden, vol. 2, 1997, paper 2ii056.
[32] C. Famy, K.L. Scrivener, A. Atkinson, A.R. Brough, Effects of an early or late heat treatment on the microstructure and composition of inner C-S-H products of Portland cement mortars, Cem. Concr. Res. 32 (2002) 269–278.
[33] I.G. Richardson, C.A. Love, 2004, private communication.
[34] S.K. Deb, M.H. Manghnani, K. Ross, R.A. Livingston, P.J.M. Monteiro, Raman scattering and X-ray diffraction study of the thermal decomposition of an ettringite-group crystal, Phys. Chem. Miner. 30 (2003) 31–38.
[35] C. Hall, P. Barnes, A.D. Billimore, A.C. Jupe, X. Turrilas, Thermal decomposition of ettringite $Ca_6[Al(OH)_6]_2(SO_4)_3{\cdot}26\ H_2O$, J. Chem. Soc., Faraday Trans. 92 (1996) 2125–2129.
[36] Q. Zhou, F.P. Glasser, Thermal stability and decomposition mechanisms of ettringite at <120 °C, Cem. Concr. Res. 31 (2001) 1333–1339.
[37] S. Merlino, E. Bonaccorsi, T. Armbruster, The real structure of tobermorite 11Å: normal and anomalous forms, OD character and polytypic modifications, Eur. J. Mineral. 13 (2001) 577–590.
[38] E. Bonaccorsi, S. Merlino, A. R. Kampf, The crystal structure of tobermorite 14Å (plombierite), a C-S-H phase, J. Am.Ceram. Soc. 88 (2005) 505–512.
[39] E. Bonaccorsi, S. Merlino, H.F.W. Taylor, The crystal structure of jennite, $Ca_9Si_6O_{18}(OH)_6{\cdot}8H_2O$, Cem. Concr. Res. 34 (2004) 1481–1488.
[40] M. Grutzeck, A. Benesi, B. Fanning, Silicon-29 magic angle spinning nuclear magnetic resonance study of calcium silicate hydrates, J. Am. Ceram. Soc. 72 (1989) 665–666.
[41] X. Cong, R.J. Kirkpatrick, ^{29}Si MAS NMR study of the structure of calcium silicate hydrate, Adv. Cem. Based Mater. 3 (1996) 144–156.
[42] H.F.W. Taylor, Sulphate reactions in concrete—microstructural and chemical aspects, Cement Technology, in: E.M. Gartner, H. Uchikawa (Eds.), Ceram. Trans., vol. 40, American Ceramic Society, Weterville, OH, USA, 1994, pp. 61–78.
[43] I.G. Richardson, G.W. Groves, The incorporation of minor trace elements into calcium silicate hydrate (C-S-H) gel in hardened cement pastes, Cem. Concr. Res. 23 (1993) 131–138.
[44] H.F.W. Taylor, Proposed structure for calcium silicate hydrate gel, J. Am. Ceram. Soc. 69 (1986) 464–467.